Medical Informatics Europe '97
C. Pappas et al. (Eds.)
IOS Press, 1997

A Model for Image Formation and Image Quality Prediction in Diagnostic Radiology

I. Kandarakis[1], D. Cavouras[1], C. Koutsourakis[1], D. Triantis[2], A. Bakas[3], G. Panayiotakis[4], C. Nomicos[2].

Departments of [1]Medical Instrumentation Technology, [2]Electronics, and [3]Radiology, Technological Educational Institution of Athens, Ag. Spyridonos Street, Aigaleo GR-122 10, Athens, Greece.
[4]Department of Medical Physics, Medical School, University of Patras, GR-265 00 Patras, Greece.

Abstract. A computer program modelling the formation of radiological images and predicting values of physical quantities that determine diagnostic image quality has been developed. The quantities are the modulation transfer function (MTF), the noise power spectrum (NPS), and the detective quantum efficiency (DQE) associated with signal to noise ratio (SNR). The program is based on mathematical models that describe the effects of x-ray interactions with the imaged object and the image detector as well as phenomena concerning the optical signal propagation within the detector. All data on x-ray effects necessary for computer calculations were derived from published work whereas optical data were determined in our laboratory using experimental techniques. Model predictions were compared with direct quality measurements performed after image formation, on the image itself.

1. Introduction

The radiographic imaging system (RIS) can be modelled as a system comprising three main sections: 1/the x-ray source (tube), 2/the object to be imaged (patient or phantom), and 3/the image receptor consisting of an x-ray to light converter (phosphor screen) and an optical sensor (film, CCD array etc.). RIS performance is assessed by several concepts such as the modulation transfer function (MTF), the noise power spectrum (NPS), the signal to noise ratio (SNR) or the detective quantum efficiency (DQE). These concepts are governed by fundamental inherent physical properties and physical processes taking place within the system [1-4]. RIS performance can be either experimentally determined by measurements on the diagnostic image or it can be predicted by computer calculations based on mathematical models describing the inherent physical phenomena in the RIS.

In this study a computer program that models the image formation process and predicts image quality in terms of MTF, NPS, and SNR was developed. Additionally, a digital image acquisition method was applied in order to experimentally determine MTF, NPS, and DQE on the final diagnostic image. Results of both experimental and theoretical processes were compared.

2. Material and Methods

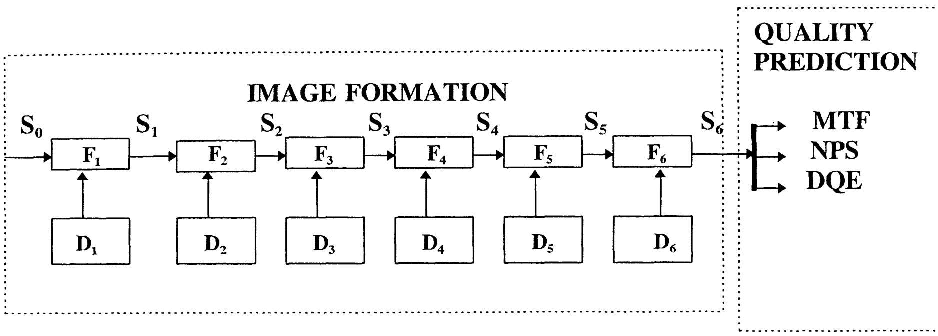

Figure 1: Schematic representation of the image formation and image quality prediction model.

The model of image formation and image quality prediction is schematically described in Figure 1. The image formation part is modelled as a six step procedure. Each step is described by a process function F_i, a set of input data D_i and an output signal S_i given by:

$$S_i=F_i(D_i) \qquad (1)$$

In the first step the output signal S_1 represents the source signal, i.e. the shape and intensity of the x-ray spectrum. The function F_1 is represented by various x-ray spectral models published in the literature [5-6]. The formulas of these models are fed with a set of data (D_1) on x-ray source characteristics obtained from manufacturers data. Specifically, D_1 is the data vector containing values for the tube target material, the angle of anode disk, and the filter material, as well as data on the tube voltage (kVp) and the tube current (mAs). In the second step, F_2 represents the interaction of the source signal S_1 with the object to be imaged. S_2 is predicted from S_1 and by feeding F_2 with data (D_2) on x-ray attenuation effects in human tissues or in phantom materials [7,8]. The third step is analogous to the second one but concerns the image receptor interaction (F_3) with the object output signal S_2. Signal S_3 is fed into the fourth step function F_4, which describes the conversion of absorbed x-ray spectrum into optical signal. S_4 corresponds to the quantity of light produced inside the x-ray to light converter. The fifth step predicts the final optical signal (S_5) transmitted to the optical sensor of the image receptor. The transmission process F_5 depends on various optical phenomena (absorption, scattering, reflection) within the material of the image receptor. The final step F_6 refers to the compatibility of the optical spectral distribution with the sensor sensitivity.

The image quality prediction part in Figure 1 comprises a series of computer calculations for predicting MTF, NPS, and DQE ($DQE=SNR^2_{input}/SNR^2_{output}$). These calculations use the previously determined output signals S_i as input data to appropriate formulas [1-4, 9]. Thus, the image receptor with optimum image quality characteristics is determined.

All data necessary for each function F_i were either obtained from the literature or were experimentally determined in our laboratory [10, 11]. The experimental procedure is divided in five sections:

1/Phosphor screen preparation from various phosphor materials (e.g., $Gd_2O_2S{:}Tb$, $La_2O_2S{:}Tb$, $Y_2O_2S{:}Tb$, $Y_2O_3{:}Eu$, $YVO_4{:}Eu$, ZnSCdS:Ag) with different coating thicknesses. The screens were prepared by sedimentation.

2/Optical measurements concerning the total optical signal emerging at screen output after x-ray excitation. This signal corresponds to the signal S_5 predicted by the model.
3/Optical measurements concerning the intrinsic x-ray to light conversion factor and the coefficients related to optical effects (light absorption, scattering and reflection) that determine functions F_4 and F_5 respectively.
4/Optical spectrum measurements were performed in order to determine the spectral compatibility of the emitted light with the optical sensor (F_6, S_6).
5/X-ray exposure measurements concerning the exposure rate necessary to produce a given optical signal intensity. This exposure rate corresponds to signal S_1.

The experimental instrumentation employed comprised photomultipliers (EMI 9558 QB) coupled to a Carry 401 or to a Keithley electrometer, a monochromator (Oriel 7240), and dosimeters (PTW Simplex, Radcal).

To test the model accuracy, direct image quality measurements were performed employing an image digitization technique. Images of a resolution test pattern (typ-53, Nuclear Associates) comprising various frequencies of line pairs per millimeter were obtained after exposing the screens to x-rays from a Phillips Medio 50CP unit. The test pattern was placed over the exposed side of the screen, the other side being in contact with the radiographic film (Agfa Curix- Ortho GS, Agfa Scopix LT2B). Pattern images were digitized via a Microtech Scan Maker II SP (24 bit color, 1200x1200 dpi) CCD scanner. Sixty four successive image traces were selected vertically to the line pairs of the pattern image. Traces were averaged to reduce noise and were normalized to the image contrast at 2.5 lp/cm. These traces constitute the Square Wave Response Function (SWRF) of the screen and they are employed in the MTF determination as follows [4, 10]:

$$MTF(v) = \frac{4}{\pi}\left[\frac{SWRF(v)}{v} + \frac{SWRF(3v)}{3v} - \frac{SWRF(5v)}{5v} + ..\right] \qquad (2)$$

where v is the spatial frequency. This MTF was divided by that of the CCD scanner in order to obtain the phosphor screen MTF. The MTF of the CCD scanner was determined by scanning the bar pattern alone. The radiographic film MTF was considered approximately equal to 1 for frequencies lower than 100 lp/cm.

Noise estimation was performed by determining the noise power spectrum (NPS) on phosphor screen digitized images obtained without the test pattern. The one-dimensional NPS was calculated by selecting a uniform area at the central region of the digitized image and by determining the auto-correlation function in the frequency domain of 128 successive image traces (noise signal) of 128 pixels in length as follows: 1/Each noise signal was multiplied by a Hanning window to taper its edges to zero; 2/The noise signal was Fourier transformed and its squared amplitude was calculated to yield the power spectrum or Wiener spectrum of each noise signal; 3/The Wiener spectra of the 128 noise signals were averaged to reduce statistical fluctuations thus yielding the Noise Power Spectrum of each screen-film combination.

The Detective Quantum Efficiency [3] was determined from experimental MTF and NPS data using relation (3):

$$DQE(v) = C^2\, MTF(v)^2 \,/\, Q(E)\, NPS(v) \qquad (3)$$

where, C is a constant related to the characteristic curve of the film-screen combination which was determined experimentally, Q(E) is the x-ray photon fluence determined from x-ray exposure measurements.

3. Results and Discussion

Figure 2 shows results on final optical signal intensity (S_5) per unit of x-ray exposure versus x-ray tube voltage and for various ZnSCdS:Ag phosphor coating thicknesses. The curves were calculated employing the image formation part of the model (see Fig. 1) and using data from section 3 of the experimental procedure as input D_5 to function F_5. In the same figure, experimental data obtained according to sections 1 and 2 of the experimental procedure are also shown (dots). From Figure 2, information concerning the type of phosphor material, the phosphor's optimum coating thickness, and the optimum high voltage for tube operation can be extracted. This kind of information is of value when the patient radiation burden for a given level of image brightness is considered. MTF and DQE results are shown in Figures 3,4,5. From Figure 3 the screen with the better spatial resolution (spatial frequency at a low MTF value) and contrast resolution (MTF at low to medium frequency range) can be seen.

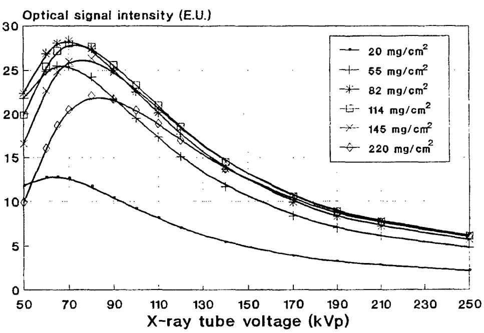

Figure 2: Optical signal intensity Vs tube voltage, predicted curves (solid lines) experimental data (dots) E.U.: 1 μW m^{-2}/mR s^{-1}

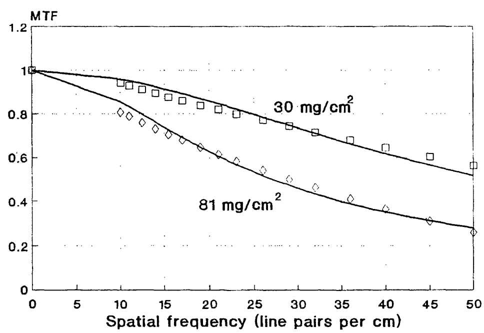

Figure 3: MTF curves predicted (solid lines) and measured (dots) of La_2O_2S:Tb phosphor screens.

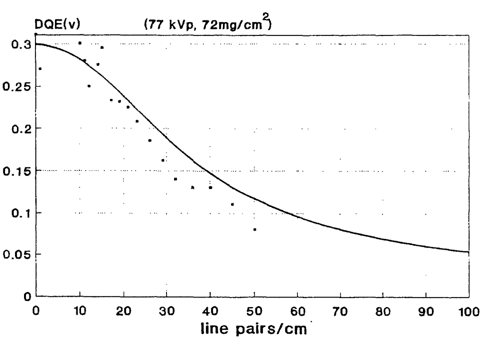

Figure 4: DQE(v) curve predicted (solid line) and measured (dots)

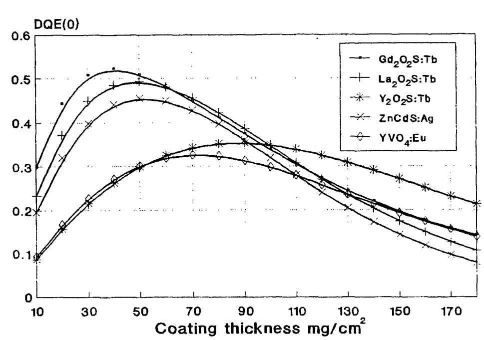

Figure 5: DQE(0) Vs coating thickness for various phosphors.

To test the validity of the model prediction, results obtained by the experimental method of SWRF measurement are also shown in Figure 3 (dots). Both methods give results that are in very good agreement to each other showing the reliability of the model calculations. A similar comparison of experimental and calculated DQEs is shown in Figure 4. The DQE curves of Figure 5 predict the type of phosphor material giving optimum signal to noise ratio at various screen coating thicknesses for a given tube voltage (25 kVp).

From the results of our model, the optimum radiographic exposure (kVp), the type of optimum screen phosphor and the screen coating thickness with optimum optical signal intensity, spatial resolution, contrast resolution and signal to noise ratio can be selected. From both experiments and model calculations it has been observed that the intensity of the final signal and the quality of the diagnostic image depend strongly on the chemical composition of the phosphor (i.e. the effective atomic number), the density, the x-ray to light conversion factor and on the coefficients expressing the optical properties of the material.

4. References

[1] G. W. Ludwig, X-ray efficiency of powder phosphors, *J. Electrochem. Soc.* **118** (1971) 1152-1159.

[2] R. K. Swank, Calculation of modulation transfer functions of x-ray fluorescent screens, *Appl. Opt.* **12** (1973) 1865-1870.

[3] J. Beutel, B. A. Apple, and R. Shaw, The role of screen parameters and print-through in the performance of film/screen systems, *Phys. Med. Biol.* **38** (1993) 1181- 1206.

[4] D. Cavouras, I. Kandarakis, G. Panayiotakis, E. Evangelou, C.Nomicos, An evaluation of the $Y_2O_3:Eu^{3+}$ scintillator for application in medical x-ray detectors and image receptors, *Med. Phys.* **23** (1996) 1965-1975.

[5] E. Storm Calculated bremsstrahlung spectra from thick tungsten targets, *Phys. Rev.* **A5** (1972) 2328-2338.

[6] D. M. Tucker, G.T. Barnes and D. P. Chakraborty, Semi-empirical model for generating tungsten target x-ray spectra, *Med. Phys.* **18** (1991) 211-218.

[7] E. Storm and H. Israel, Photon cross-sections from 0.001 to 100 MeV for elements 1 through 100 *Report LA-3753* Los Alamos Scientific Laboratory of the University of California, 1967.

[8] P.C. Johns and M. J. Yaffe, X-ray characterization of normal and neoplastic breast tissue, *Phys. Med. Biol.* **32** (1987) 675-695.

[9] R. M. Nishikawa and M. J. Yaffe, Model of the spatial-frequency-dependent detective quantum efficiency of phosphor screens, *Med. Phys.* **17** (1990) 894-904.

[10] I. Kandarakis, D. Cavouras, G. Panayiotakis, T. Agelis, C. Nomicos, G. Giakoumakis, x-ray induced luminescence and spatial resolution of La_2O_2S:Tb phosphor screens, *Phys. Med. Biol.* **41** (1996) 297-307.

[11] G. Panayiotakis, D. Cavouras, I. Kandarakis, C. Nomicos, A study of X-ray luminescence and spectral compatibility of europium-activated yttrium-vanadate (YVO_4:Eu) screens for medical imaging applications, *Appl. Phys.* **62** (1996) 483-486.

Address for correspondence:
Prof. D. Cavouras,
37-39 Esperidon Street,
Kallithea 17671, Athens, Greece
e-mail: cavouras @ hol.gr
fax: +301-9594-558 (home), (+301) 5910 975 (work).